Combined Wavelet Transform with Curve-fitting for Objective Optimization of the Parameters in Fourier Self-deconvolution

ZHANG, Xiu-Qi(张秀琦) ZHENG, Jian-Bin*(郑建斌) GAO, Hong(高鸿)
Institute of Electroanalytical Chemistry, Northwest University, Xi'an, Shaanxi 710069, China

Fourier self-deconvolution was the most effective technique in resolving overlapping bands, in which deconvolution function results in deconvolution and apodization smoothes the magnified noise. Yet, the choice of the original half-width of each component and breaking point for truncation is often very subjective. In this paper, the method of combined wavelet transform with curve fitting was described with the advantages of an enhancement of signal to noise ratio as well as the improved fitting condition, and was applied to objective optimization of the original half-widths of components in unresolved bands for Fourier self-deconvolution. Again, a noise was separated from a noisy signal by wavelet transform, therefore, the breaking point of apodization function can be determined directly in frequency domain. Accordingly, some artifacts in Fourier self-deconvolution were minimized significantly.

Keywords Fourier self-deconvolution, wavelet transform, curve fitting, parameter estimation, resolving overlapping bands

Introduction

Fourier self-deconvolution (FSD) was originally developed by Kauppinen *et al*.[1-3] and most commonly used in resolving overlapping spectroscopy. The main purpose of FSD for resolving overlapping bands is to reduce the full width at half height ($w_{1/2}$) to the point that each component can be recovered or resolved from the multiplets whereas the peak position and peak area remain constant before and after deconvolution. Nevertheless, the main disadvantage of FSD is that the choice of the original $w_{1/2}$ of each component and breaking point for truncation is often very subjective and, if incorrect, can lead to generation of artifacts in the spectrum after FSD. To obtain objective and quantitative information, these parameters need to be optimized to give a maximum achievable resolution enhancement without an introduction of negative side lobes or excessive noises, both of which will mask real weak spectral features. One method for doing this was previously suggested by Yang and Griffiths.[4,5] Rahmelow *et al*.[6] described an objective method to obtain the starting parameters and breaking point for truncation. Laszlo[7] provided a straightforward method to determine the appropriate parameters.

Curve fitting[8-11] program is a very useful optimization technique and has been employed to many kinds of optimization due to its good precision. Yet, it usually yields accurate parameters for unresolved spectra only when the number of unresolved bands and peak positions of each band in the multiplet can be estimated with much improved accuracy. Accordingly, many kinds of methods have been applied to improve the fitting conditions.[12-19] In this work, wavelet transform-based curve fitting was proposed. Here wavelet transform was used prior to curve fitting in order to enhance the signal to noise ratio (*SNR*) as well as to improve the fitting conditions by supplying two essential factors of peak number and peak position, then curve fitting was applied to optimize the parameters used in FSD. In addition, wavelet transform was used to decompose the signals into higher frequency (noises) and lower frequency components (denoised signals) according to its frequency distribution. Then, the breaking point (L) in apodization function can be determined accordingly in frequency domain. As a conse-

* E-mail: zhengjb@nwu.edu.cn
Received December 22, 2000; revised and accepted May 18, 2001.
Project supported by the National Natural Science Foundation of China (No. 29775018).

quence, some artifacts in FSD were minimized because of an objective estimation of parameters in FSD.

Theory

Fourier self-deconvolution

Any experimental signal, $f(t)$, can be expressed as a convolution of a lineshape function, $g(t)$, with a higher-resolution signal, $f'(t)$, that is

$$f(t) = g(t) * f'(t) = \int_{-\infty}^{+\infty} (t-\tau) \cdot f'(t) \mathrm{d}\tau \quad (1)$$

where * indicates convolution operation. Provided that the Fourier transform of $f(t)$, $g(t)$ and $f'(t)$ exist, a solution of Eq.(1) may be obtained in the form

$$f'(t) = \zeta^{-1}\left\{\frac{F(\omega) \cdot D(\omega)}{G(\omega)}\right\} \quad (2)$$

here $\zeta^{-1}\{\}$ is the inverse Fourier transform. $F(\omega)$, $D(\omega)$ and $G(\omega)$ are frequency features of $f(t)$ function, apodization function $d(t)$ and lineshape function $g(t)$, respectively. There are a large number of possible apodization functions, triangular, triangular squared, bessel, cos, $\sin^2$ *etc*. The only major constraint is that there is a very small value for $|t| > L$, that is

$$d(t, L) = \zeta^{-1} d(\omega) = \begin{cases} d(t), & |t| < L \\ 0, & |t| > L \end{cases} \quad (3)$$

From Eq.(2), it is apparent that the deconvoluted signal is determined mainly by lineshape function and apodization function. Lineshape function results in deconvolution but yields magnified noises whereas apodization function smoothes the magnified noises but at the cost of resolution enhancement. Clearly, the choice of a proper $w_{1/2}$ of lineshape function and a proper breaking point for trunction is essential to achieve higher resolution enhancement as well as lower noise level. However, the choice of these parameters is still subjective.

Combined wavelet transform with curve fitting

Wavelet transform is becoming an increasingly important tool in image and signal processing. It is effective in extraction of both time- and frequency-like information from a time-varying signal. Therefore, it has been used to resolving overlapping bands[20-25] and peak finding.[26]

If an analytical signal is assumed to be a time order signal, its discrete form at the j-th scale is given by[27]

$$A_{2j}f(n) = \sum_{k=1}^{l} h(k) * A_{2j-1}f(n - 2^j k) \quad (4)$$

$$D_{2j}f(n) = \sum_{k=1}^{l} g(k) * A_{2j-1}f(n - 2^j k) \quad (5)$$

where $A_{2j}f(n)$ and $D_{2j}f(n)$ are called the discrete approximation and the discrete detail, respectively. $h(k)$ and $g(k)$ are discrete low-pass filter and high-pass filter respectively corresponding to a pair of sequence $\{h_k\}$ and $\{g_k\}$.

Noise is a phenomenon that affects all frequencies, whereas the signal of interest is most likely to occupy a small part of the frequency domain. Because the signal will tend to dominate the low-frequency components, it is expected that the majority of high-frequency components above a certain level is due to noises. This is the underlying philosophy for traditional Fourier filtering where low-pass filters cut off the high-frequency components. Similarly, small wavelet coefficients at short scales can be expected to be mainly noisy components. Thus to some details such as D_1 and D_2, they mainly consist of noises whereas to a certain detail such as D_3 or D_4, it can represent the main information of the signal. Therefore, the peak number as well as peak position of individual components in unresolved bands can be obtained from some of these details, and this is determined by the frequency distribution of both useful information and noise.[28] To a certain discrete approximation A^j, its noise level is much lower than the original signal due to that a majority of noise is deducted from the original signal. Then, a noisy signal can be represented as:

$$f^{\mathrm{noisy}}(t) = f^{\mathrm{denoised}}(t) + n(t) = A^j(t) + \sum_{j=1}^{n} d^j(t) \quad (6)$$

where, $A^j(t)$ and $\sum_{j=1}^{n} d^j(t)$ at a short scale can approximately represent denoised signal $f^{\mathrm{denoised}}(t)$ and noises $n(t)$, respectively.

The frequency spectra of denoised signal can be obtained by performing Fourier transform on the denoised signal $A^j(t)$

$$A^j(\omega) = \int_{-\infty}^{+\infty} A^j(t)\exp(-i\omega t)\mathrm{d}t = \zeta\{A^j(t)\} \quad (7)$$

Similarly, the frequency spectra of noise $\sum_{j=1}^{n} d^j(t)$ can be obtained as follows:

$$D^j(\omega) = \int_{-\infty}^{+\infty} d^j(t)\exp(-i\omega t)\mathrm{d}t = \zeta\{\sum_{j=1}^{n} d^j(t)\} \quad (8)$$

The frequency spectra of denoised signal and noise are divided by lineshape function in frequency domain to result in deconvolution. Thus, the deconvoluted denoised signal and deconvoluted noise signal can be obtained as follows:

$$A'^j(\omega) = \frac{A^j(\omega)}{G(\omega)}, \quad D'^j(\omega) = \frac{D^j(\omega)}{G(\omega)} \quad (9)$$

With the increase of the frequency, $A'^j(\omega)$ is an exponential decay function whereas $D'^j(\omega)$ is an increase function. Thus, the breaking point L is determined at the equal amplitude of $A'^j(\omega)$ and $D'^j(\omega)$.

As discussed before, the main advantages of performing wavelet transform on a signal are an enhancement of signal to noise ratio and the knowledge of peak number and peak position. On basis of this, good parameters of components in unresolved bands could be achieved by curve fitting the denoised data under the improved fitting condition.

Experimental

Several various spectra were synthesized from more Lorentzian peaks to investigate the potential advantages of this method for parameter estimation. Moderate amounts of noises were added to all these synthesized spectra. Table 1 lists parameters used to synthesize these spectra.

Table 1 Parameters of synthetic bands discussed in this paper

Parameter	Spectrum A			Spectrum B			Spectrum C				Spectrum D			
	I	II	III	I	II	III	I	II	III	IV	I	II	III	IV
Position	240	255	270	235	255	270	220	242	262	286	220	240	265	288
$w_{1/2}$	15	15	15	25	20	15	25	25	25	25	20	30	35	25
Area	0.6	1.2	0.6	1.0	1.2	1.5	1.5	2.0	1.7	1.4	2.0	1.8	2.2	1.5

Results and discussion

Estimation of $w_{1/2}$ of components in unresolved bands

From the theory, it is clear that sidelobes and magnified noises result from improper $w_{1/2}$ in lineshape function. If the selected lineshape is narrower than the experimental one, it may result in under-deconvolution with lower resolution enhancement. Otherwise, it may lead to over-deconvolution with negative sidelobes and magnified noises. In theory, the $w_{1/2}$ in lineshape function for deconvolution should be equal to that of the original overlapping bands if the $w_{1/2}$ is equal in unresolved bands. Otherwise, it should be the same of the narrowest component so as to avoid distortion from overdeconvolution. Clearly, the choice of $w_{1/2}$ in lineshape function means to determine the original $w_{1/2}$ of unresolved bands.

For clarity of presentation, this work first delt with a simulated spectrum A (Fig. 1a) in the absence of noise. First, the spectrum A was decomposed into discrete approximation and discrete details with Haar wavelet. To some details (D_2, D_3 or D_4), it can supply the peak number and peak positions of unresolved bands (Fig. 1b). Then, with these two parameters, the original bands are fitted to give an estimation of $w_{1/2}$. Finally, with the estimated $w_{1/2}$, the deconvoluted band was shown in Fig. 1c.

To further investigate the advantages of the method for estimation of original $w_{1/2}$, four various spectra were synthesized from more Lorentzian bands. Since main advantage was expected to be a very accurate $w_{1/2}$ estimation, all spectra contained in Table 1 were discussed firstly without an introduction of noise and relative error ($E\%^a$) of $w_{1/2}$ estimation was presented in Table 2. Clearly, $E\%^a$ is less than 0.5% when a resolution (de-

fined as $R_s = \frac{2\times(x_1 - x_2)}{w_1 + w_2}$, where, x_1, x_2 and w_1, w_2 are peak positions and $w_{1/2}$ of neighboring bands, respectively) of neighboring bands is higher than 0.5. When a resolution is below 0.4 and the number of unresolved peaks is less than 4, the relative error is not higher than 2%.

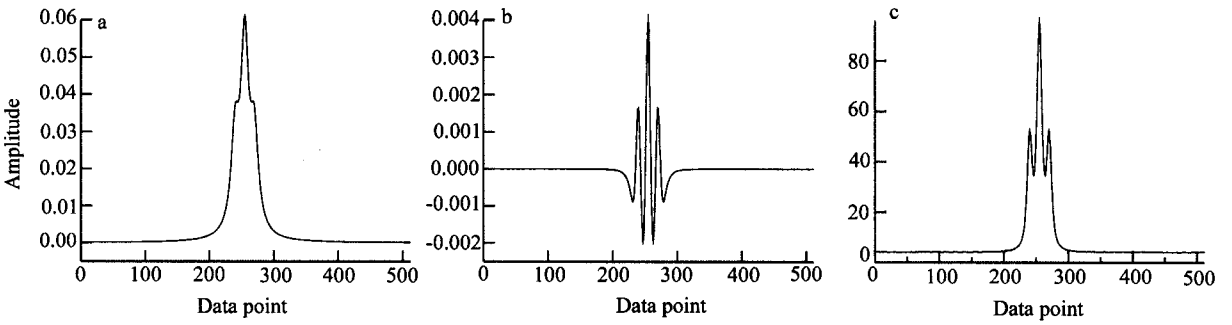

Fig. 1 Procedure for the estimation of $w_{1/2}$ (a: original spectra; b: detail D_3 obtained from wavelet transform; c: deconvoluted spectrum with estimated $w_{1/2}$).

Effects of noises on the estimation of $w_{1/2}$

However, almost all realistic spectra include a certain mount of noise. So, moderate mount of noise was introduced to all these spectra contained in Table 1 to investigate an effect of noise on the accuracy of $w_{1/2}$ estimation. In Table 2, $E\%^b$ and $E\%^c$ represent the relative error of $w_{1/2}$ of these spectra with signal to noise ratio *SNR* approximately equal to 100 and 50 respectively. In comparison of $E\%^b$ and $E\%^c$ with $E\%^a$, it is apparent that the accuracy of band estimation is not seriously affected by the noise level if the *SNR* is not less than 100. But it decreases highly as *SNR* decreases if the *SNR* is lower than 100 even when a resolution of neighboring bands is not less than 0.5. This is because noise is normally distributed, curve fitting not only yields a statistically valid solution but it can also be shown to yield the maximum likelihood solution. In addition, the error derived from a shift of peak position caused by implementing wavelet transform on original spectra is negligible too. In contrast, when the noise levels are very high, the presence of noise may not only lead to fitted errors but also result in a bigger shift of peak position which yields fitted errors in turn, especially those bands with lower relative intensity. In Table 2, $E\%^d$ represents the relative error of $w_{1/2}$ for an appropriate approximation to be fitted which was obtained from performing wavelet transform on the spectra with the same *SNR* as what $E\%^c$ represents. It can be drawn from the comparison of $E\%^c$ and $E\%^d$ that satisfactory estimations can be acquired if an appropriate approximation (A^2) was used to be fitted for the estimation rather than the original spectra were used when noise level was high. This is presumably because the approximation has higher *SNR* than the original spectra.

Table 2 Estimation of $w_{1/2}$ of components in unresolved bands with the method

Error	Spectrum A			Spectrum B			Spectrum C				Spectrum D			
(%)	I	II	III	I	II	III	I	II	III	IV	I	II	III	IV
$E\%^a$	0.2	-0.1	0.1	0.0	-0.1	0.0	0.0	-0.2	0.2	-0.1	0.0	0.0	-0.1	0.0
$E\%^b$	2.4	1.1	1.6	3.6	2.3	0.2	3.1	2.1	1.6	1.9	-4.0	14	0.1	0.2
$E\%^c$	5.3	2.0	3.3	8.8	2.5	0.1	6.0	4.4	1.2	4.0	-7.0	24	3.7	-1.6
$E\%^d$	4.0	2.7	2.2	4.8	6.5	2.7	5.6	5.2	-2.4	5.6	4.9	18	0.6	9.2

Effects of resolution on the estimation of $w_{1/2}$

Curve-fitting program usually only yields accurate parameters for unresolved spectra when the separation of neighboring bands exceeds their average $w_{1/2}$. Thus, the degree of separation has also influence on the accura-

cy of $w_{1/2}$ estimation. A set of spectra with different resolution but equal *SNR* of about 120, which comprised three Lorentzian lines with relative intensities of 6, 8 and 10, was synthesized to investigate the influence of resolution on the accuracy of $w_{1/2}$ estimation. Table 3 lists relative errors caused by resolution. In the Table 3, $E\%^a$ *etc*. represent the relative error when resolutions of neighboring bands are 0.4, 0.5, 0.6, 0.7 and 0.8, respectively. It is evident that the resolution also has significant influence on the estimation of $w_{1/2}$ and the relative error increases with the increase of the degree of overlapping.

From the above discussion it can be seen that both noise level and the degree of overlapping affect the accuracy of an estimation of the $w_{1/2}$. However, the relative errors are in the range of -8.5%—$+11.5\%$ which may not result in unacceptable pseudo-deconvolution. This can be illustrated by using spectrum A with the original $w_{1/2}$ of σ_0. Fig. 2 shows the comparison of deconvoluted results when the $w_{1/2}(\sigma_0)$ of lineshape function is 0.88, 1 and 1.15-fold of that of original $w_{1/2}$ (σ_0) respectively, *i.e.* $\sigma = 0.88\sigma_0$ (Fig. 2a), $\sigma = \sigma_0$ (Fig. 2b), and $\sigma = 1.15\sigma_0$ (Fig. 2c). From the Fig. 2 it can be seen that pseudo-deconvolution could be precluded at the furthest extent in this relative error ranges. Obviously, when this method is applied to estimate the original $w_{1/2}$ of components in unresolved bands, the deconvoluted condition could be enhanced to the point that pseudo-deconvolution may be precluded at the furthest extent.

Table 3 Effect of the resolution on the accuracy of $w_{1/2}$ estimation

		$w_{1/2}$	$E\%^a$	$E\%^b$	$E\%^c$	$E\%^d$	$E\%^e$
Spectrum	I	30.0	2.0	10.8	9.6	8.0	5.6
	II	25.0	11.6	1.2	−0.2	1.6	0.8
	III	20.0	−8.5	1.5	0.1	0.5	1.0

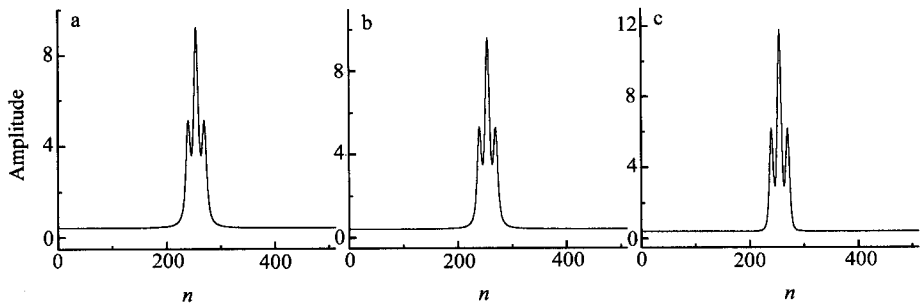

Fig. 2 Study of the effects of different $w_{1/2}$ in the lineshape function (a: $\sigma = 0.88\sigma_0$; b: $\sigma = \sigma_0$; c: $\sigma = 1.15\sigma_0$).

Determination of cutoff frequency

The aim of self-deconvolution is to separate overlapping bands by making them narrower. Nonetheless, experimental spectra were always contaminated by some noises, which unfortunately exponentially increase during the procedure of deconvolution and therefore limit the resolution enhancement. Thus an apodization function was needed to reduce noises and some negative side lobes. To a certain apodization function, breaking point, L, is a crucial parameter to determine the effectiveness of smoothing. In theory, the breaking point would be optimal to select a value for L that is as large as possible, corresponding to the lower noise level and smaller side lobes of the deconvoluted spectrum. However, in practice the increase of L would lead to the decrease of resolution enhancement factor. As a consequence, an appropriate L should be chosen to attain higher resolution enhancement and lower noise level and side lobes. Here, the procedure is illustrated for determining L in this work as follows:

$$f^{\text{noisy}}(t) = \xrightarrow{\text{wavelet transform}} \begin{cases} f^{\text{denoised}}(t) \approx A^j(t) \xrightarrow{\text{FFT}} A^j(\omega) \xrightarrow{/G(\omega)} A'^j(\omega) \longrightarrow L: A'^j(\omega) = D'(\omega) \\ n(t) \approx \sum D^j(t) \xrightarrow{\text{FFT}} D(\omega) \xrightarrow{/G(\omega)} D'(\omega) \end{cases}$$

To an experimental signal $f^{noisy}(t)$, it consists of two portions of signal $f^{denoised}(t)$ and noise $n(t)$. Yet, the signal of interest is most likely to occupy a small part of the frequency domain. Because the signal will tend to dominate the low-frequency components, it is expected that the majority of high-frequency components above a certain level is mainly noise. Therefore, a noisy signal could be decomposed into two parts with wavelet transform: denoised signal $A^j(t)$ and noises $\sum_{j=1}^{j} D^j(t)$. Then the spectra of both denoised signal and noises can be achieved by Fourier transform and they are divided by lineshape function in the Fourier domain array. Thus, the amplitude of noises increases exponentially whereas the amplitude of signal decays to a very small value as the spatial frequency increases. In this case inclusion of signal at higher spatial frequencies only serves to increase the noise level in the spectrum without significantly increasing the available information and it may be further truncated without introducing side lobes into the deconvoluted spectra. It is apparent that to achieve optimal filtering the part need be cut where the amplitude of noise is bigger than the signal. This procedure can be illustrated explicitly by using outline of the FSD procedure in the time domain and frequency domain with Fig. 3.

In the oscillographic chonopotentiometry, the determination is based on the relationship between the concentration of samples and the depth of incision on the dE/dt vs. t curve. As shown in Fig. 3a, the incision, based on the dE/dt vs. t curve of Cd^{2+} and In^{3+} in 0.5 mol/L NH_4OAc solution, can be viewed as the result generated by two neighboring overlapped peaks. Thus, its depth can be increased by deconvoluting these overlapping peaks. By performing wavelet transform on the noisy dE/dt vs. t curve, it would be decomposed into two parts of the denoised signal (Fig. 3b) and noises (Fig. 3c) under a certain scale factor ($j = 2$). Fig. 3d shows the spectra of these two parts divided by lineshape function in frequency domain. From Fig. 3d it can be seen that L can be determined very easily. Fig. 3e shows the deconvoluted spectrum without apodization while Fig. 3f represents the deconvoluted spectrum smoothed with Bessel function with L obtained from Fig. 3d. It is very evident from a comparison of Fig. 3e and Fig. 3f that the noise level is much lower after apodization but at almost the same resolution enhancement factor.

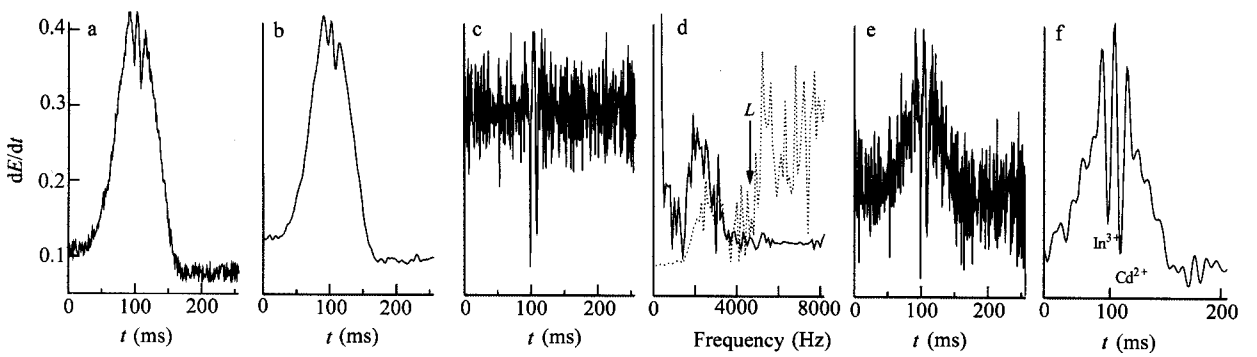

Fig. 3 Outline of the procedure for determination of L [a: dE/dt vs. t curve of $f^{noisy}(t)$, b: an approximation $A^2(t)$, c: noise $n(t)$, d: frequency spectra of $A^2(\omega)$, and $N(\omega)$, e: deconvoluted spectrum without apodization, f: deconvoluted spectrum after apodization].

Conclusion

The objective of this paper is an exposition of the method of combined wavelet transform with curve fitting for an objective estimation of $w_{1/2}$ of components in unresolved bands for FSD. Also, the procedure for the determination of breaking point of apodization function by using wavelet transform to decompose a signal into a denoised signal (approximation) and noises was described. From the above discussion, it is very evident that the method should allow objective optimization of the parameters used in FSD. Consequently, some drawbacks could be easily precluded. To some extent, higher resolution enhancement factor can be achieved presumably due to appropriate parameters for FSD and the use of denoised spectrum for further deconvolution.

References

1 Kauppinent, J. K.; Moffatt, D. J.; Mantsch, H. H.; Cameron, D. G. *Appl. Spectrosc.* **1981**, *35*, 271.

2 Kauppinent, J. K.; Moffatt, D. J.; Mantsch, H. H.; Cameron, D. G. *Anal. Chem.* **1981**, *53*, 1454.

3 Kauppinent, J. K.; Moffatt, D. J.; Mantsch, H. H.; Cameron, D. G. *Appl. Opt.* **1981**, *20*, 1866.

4 Yang, W. J.; Griffiths, P. R. *Comput. Enhanced Spectrosc.* **1983**, *1*, 157.

5 Yang, W. J.; Griffiths, P. R. *Comput. Enhanced Spectrosc.* **1984**, *2*, 69.

6 Rahmelow, K.; Húbner, W. *Appl. Spectrosc.* **1996**, *50*, 795.

7 László, S.; Goossens, K.; Heremans, K. *Appl. Spectrosc.* **1995**, *49*, 1538.

8 Young, R. P.; Jones, R. N. *Chem. Rev.* **1971**, *71*, 219.

9 Antoon, M. K.; Koenig, J. H.; Koenig, J. L. *Appl. Spectrosc.* **1977**, *31*, 518.

10 Painter, P. C.; Rimmer, S. M.; Synder, R. W.; Davis, A. *Appl. Spectrosc.* **1981**, *35*, 102.

11 Gold, H. S.; Rechsteiner, C. E.; Buck, R. P. *Anal. Chem.* **1976**, *48*, 1540.

12 Maddams, W. F.; Mead, W. L. *Spectrochim. Acta*, **1982**, *38A*, 437.

13 Griffiths, T. R.; King, K. *Anal. Chim. Acta* **1982**, *193*, 163.

14 Jackson, R. S.; Griffiths, P. R. *Anal. Chem.* **1991**, *63*, 2557.

15 Pierce, J. A.; Jackson, R. S.; van Every, K. W.; Griffiths, P. R.; Hongjin, G. *Anal. Chem.* **1990**, *62*, 477.

16 Wythoff, B. J.; Levine, S. E.; Tomellini, S. A. *Anal. Chem.* **1990**, *62*, 2702.

17 Callant, S. R; Fraleigh, S. P.; Cramer, S. M. *Chemom. Intell. Lab. Syst.* **1993**, *18*, 41.

18 De Weiler, A. P.; Lucaslus, C. B. *Anal. Chem.* **1994**, *66*, 23.

19 Zhang, X. Q.; Zheng, J. B.; Gao, H. *Analyst* **2000**, *125*, 915.

20 Zheng, X. P.; Mo, J. Y. *Sci. China* (*Ser.* B) **1999**, *29*, 141.

21 Zhang, Y. Q.; Mo, J. Y.; Xie, T. R.; Cai, P. X. *Analyst* **2000**, *125*, 1303.

22 Bakshi, B. R. *J. Chemom.* **1999**, *13*, 415.

23 Shao, X. G.; Cai, W. S.; Sun, P. Y. *Anal. Chem.* **1997**, *69*, 1722.

24 Shao, X. G.; Hou, S. Q. *Anal. Sci.* **1999**, *15*, 681.

25 Shao, X. G.; Hou, S. Q. *Anal. Lett.* **1999**, *32*, 2507.

26 Shao, X. G.; Cai, W. S.; Sun P. Y. *Chemom. Intell. Lab. Syst.* **1998**, *43*, 147.

27 Grossmann, A.; Morlet, J. *SIAM J. Math. Anal.* **1984**, *15*, 723.

28 Zhang, X. Q.; Zheng, J. B.; Gao, H. *Anal. Chim. Acta* in press.

(E200012283 JIANG, X.H.; LING, J.)